

Luminescence of coupled quantum wells: Effects of indirect excitons in high in-plane magnetic fields

M. Orlita,* R. Grill, and M. Zvára

Institute of Physics, Charles University, Ke Karlovu 5, CZ-121 16 Prague 2, Czech Republic

G. H. Döhler and S. Malzer

Institute für Technische Physik I, Universität Erlangen-Nürnberg, D-91058 Erlangen, Germany

M. Byszewski

Grenoble High Magnetic Field Laboratory, Boîte Postale 166, F-38042 Grenoble Cedex 09, France

J. Soubusta

Joint Laboratory of Optics, Palacký University, 17. listopadu 50, CZ-772 07 Olomouc, Czech Republic

(Received 19 January 2004; revised manuscript received 5 April 2004; published 20 August 2004)

Luminescence measurements of a $\text{Ga}_{1-x}\text{Al}_x\text{As}/\text{GaAs}$ double quantum well in in-plane magnetic fields up to 22 T are reported. The properties of spatially direct and indirect excitons are studied. We show that the strong indirect exciton luminescence survives in samples with low nonradiative recombination up to high in-plane magnetic fields. This contrasts with previously published results, where its strong suppression, observed for magnetic fields as low as of 10 T, was explained by the exciton center-of-mass momentum conservation. We attribute the discrepancy to a relatively low nonradiative recombination in the studied sample in comparison with the radiative recombination of localized indirect excitons.

DOI: 10.1103/PhysRevB.70.075309

PACS number(s): 78.67.De, 78.55.Cr, 73.21.Fg, 71.35.-y

I. INTRODUCTION

Double quantum well (DQW) represents a structure that allows for the study of basic quantum phenomena in the transition from two- (2D) to three-dimensional (3D) systems. In particular, a lot of attention has been paid to excitons, i.e., to the coupled electron-hole excitations. The DQW enables the formation of a spatially indirect exciton (IX) when an electron and a hole are located in opposite wells. The spatial separation leads to their very long lifetimes,^{1,2} usually 3 orders of magnitude longer than for intrawell (direct) excitons (DX). Another special feature of excitons is their bosonic character. Thus, the gas of free excitons behaves according to Bose-Einstein statistics and in the case of long-living IXs a transition to a Bose-Einstein condensate is predicted at low temperatures. Recent experiments^{1,2} in this field are very promising.

The spatial separation of electrons and holes in different wells leads in the in-plane magnetic field B_{\parallel} to a shift of the IX ground state to a finite center-of-mass (CM) momentum in k space. Thus, the IX becomes indirect in the real, as well as in the reciprocal, space. The exciton dispersion in the DQW plane remains parabolic, but its minimum is displaced. For the magnetic field $\mathbf{B}=(0, B_{\parallel}, 0)$ with the gauge $\mathbf{A}=(B_{\parallel}z, 0, 0)$ we get the indirect exciton dispersion,

$$E(K_x, K_y) = E_0 + \frac{\hbar^2}{2M} \left[\left(K_x - \frac{eB_{\parallel}d}{\hbar} \right)^2 + K_y^2 \right], \quad (1)$$

where d represents the center-to-center distance of wells when the intrawell Stark effect is neglected. E_0 and M denote the IX energy at rest and its in-plane mass, respectively, and

e is the electron charge. For many experimental conditions, the Boltzmann statistics can be used for the description of the IX gas, instead of the Bose-Einstein distribution. Taking account of this assumption, the density of IX with CM momentum $K \approx 0$ decreases as a Gaussian function of the in-plane magnetic field: $\exp(-e^2 d^2 B_{\parallel}^2 / 2Mk_B T)$, where k_B is Boltzmann constant and T represents the IX gas temperature. Owing to the conservation of the particle's momentum, only the excitons with $K \approx 0$ can be optically active and thus the IX radiative recombination is strongly suppressed by the in-plane magnetic field. This effect was discussed theoretically by Gorbatsevich and Tokatly.³ Simultaneously, the energy of IX optical transitions increases quadratically with the magnetic field by the amount of $e^2 d^2 B_{\parallel}^2 / 2M$. This simple model was used by Parlangei *et al.*⁴ to explain their photoluminescence (PL) measurements.⁵ The authors observed the quadratic shift of the IX energy and the Gaussian suppression of the IX PL intensity with the magnetic field, and achieved a very good quantitative agreement between the simple theory and their experiment. However, the Gaussian quenching of the IX PL intensity is based on an assumption that the IX density remains unaffected by B_{\parallel} , and this is fulfilled only when the nonradiative recombination is dominant and independent of the magnetic field. Otherwise, the IX density has to increase with magnetic field, i.e., together with a decrease of the radiative recombination probability of the free IXs. The simple model is then no more valid and the IX PL intensity is governed by the variation of the radiative, as well as the nonradiative, decay rates. The IX luminescence in in-plane magnetic fields was also studied by Butov *et al.*⁶ Even though the paper is primarily devoted to the time-resolved IX

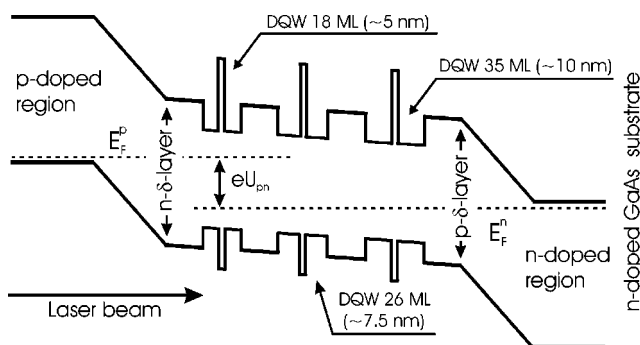


FIG. 1. The schematic picture of a sample studied under the typical operational condition $U_{pn} < 0$. E_F^p and E_F^n denote Fermi level in p - and n -doped regions, respectively. Lengths are not in scale.

photoluminescence, the quadratic shift of IX energy was evaluated from time-integrated PL spectra according to $e^2 d^2 B_{\parallel}^2 / 2M$. Also the strong IX PL quenching was clearly observed and qualitatively described.

II. EXPERIMENT

The PL measurements were carried out on a $\text{Ga}_{1-x}\text{Al}_x\text{As}/\text{GaAs}$ sample schematically depicted in Fig. 1, and prepared by molecular-beam epitaxy. The growth started on an n -doped substrate at a temperature of 600 °C with a 500-nm-wide n -doped GaAs region (Si, $1.4 \times 10^{18} \text{ cm}^{-3}$) followed by n -doped and intrinsic $\text{Ga}_{0.7}\text{Al}_{0.3}\text{As}$ layers with thicknesses of 300 and 500 nm, respectively. The growth was continued with a 5-nm-thick p - δ layer (C, $3 \times 10^{17} \text{ cm}^{-3}$) and 100 nm of an intrinsic region, both from $\text{Ga}_{0.7}\text{Al}_{0.3}\text{As}$. Afterwards, three symmetric GaAs DQWs separated always by 100 nm of $\text{Ga}_{0.7}\text{Al}_{0.3}\text{As}$ layers were added. Each DQW consists of 4 ML (ML=atomic monolayer) of AlAs central barrier separating two quantum wells with the same width of 35, 26, or 18 ML, respectively. Further $\text{Ga}_{0.7}\text{Al}_{0.3}\text{As}$ layers were grown as follows: 100-nm intrinsic, 5-nm n - δ layer (C, $4 \times 10^{17} \text{ cm}^{-3}$), 500-nm intrinsic, and 300-nm p doped (C, $1.4 \times 10^{18} \text{ cm}^{-3}$). The structure was closed by a 20-nm-wide p -doped (C, $2 \times 10^{18} \text{ cm}^{-3}$) GaAs cap. The sample was photolithographically processed, i.e., the structure was mesa etched isolated and selectively contacted to the bottom n and top p regions. Hence, the DQWs can be tilted by the perpendicular electric field when a bias is applied to these contacts. Taking account of the distance of 1.45 μm between the p and n contacts, the bias change of $\Delta U_{pn} = 1 \text{ V}$ represents the change of the electric field 6.9 kV/cm on the DQW. The compensating δ layers allow us to achieve a DQW flatband position for a relatively small bias voltage.

The sample was excited by a Ti:sapphire laser with the power density $\sim 100 \text{ mW/cm}^2$ at the photon energy 1.75 eV, i.e., below the band gap of $\text{Ga}_{0.7}\text{Al}_{0.3}\text{As}$ at low temperature. Fiber optics were used for the excitation, as well as for the signal collection. The PL spectra were analyzed by a single-grating monochromator and detected by a cooled charge coupled camera. The helium bath cryostat that we used

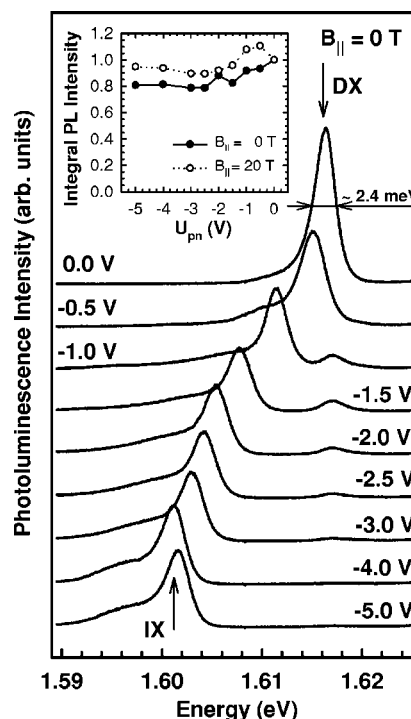


FIG. 2. PL spectra for selected negative bias at zero magnetic field. The corresponding voltages are indicated. The inset depicts integral PL intensity vs applied bias for $B_{\parallel} = 0$ and $B_{\parallel} = 20 \text{ T}$. The values in the inset are normalized to zero bias for both magnetic fields.

ensured a good temperature stability at 4.2 K. All measurements were performed in a resistive solenoid in the Voigt configuration up to the magnetic field of 22 T.

III. RESULTS AND DISCUSSION

Figure 2 shows the PL spectra for selected values of bias U_{pn} taken at $B_{\parallel} = 0$. The depicted spectra, as well as others presented in this paper, are related to the 18-ML-wide ($\approx 5 \text{ nm}$) DQW only. The remaining wells exhibited similar results. The applied U_{pn} tilts the DQW and a characteristic redshift of IX (interwell) transition for the increasing negative bias is observed, whereas the DX energy remains almost unaffected. These results are analogous to those published previously,⁷ where PL of the same structure was studied at higher temperatures. The flatband regime was observed for a small forward bias $U_{pn} \approx +0.5 \text{ V}$, where more complex PL spectra were obtained, probably related to the formation of charged excitons-trions (not shown in this paper). These charged complexes were also identified in the PL spectra of the 35-ML ($\approx 10 \text{ nm}$) DQW in this sample under different experimental conditions.⁸ For the bias in the range of $-3.0 \text{ V} < U_{pn} < -1.0 \text{ V}$, both IX and DX transitions are present in the PL spectra. The IX redshift is saturated for $U_{pn} < -4.0 \text{ V}$. This effect can be explained by a screening of the external electric field caused by IXs with sufficiently high density n_{IX} . The fact that this saturation point appears in different DQWs for other bias U_{pn} , and that the energy of the

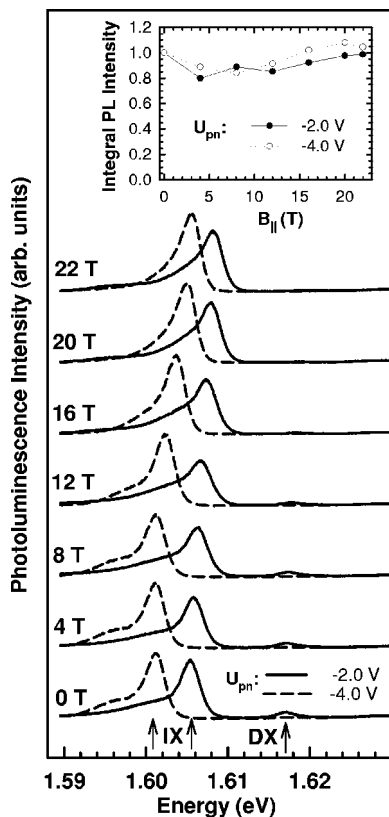


FIG. 3. The PL spectra in the dependence on the in-plane magnetic fields $B_{||}$ for two selected biases, -2.0 and -4.0 V. The corresponding fields $B_{||}$ are depicted near the curves. The inset shows the total PL intensity; values are normalized to zero magnetic field. The temperature was $T_{bath}=4.2$ K.

IX transition strongly depends on excitation intensity (not shown in this paper), supports this interpretation. The simple formula for the electric field in a plate capacitor $en_{IX}/\epsilon_0\epsilon_r$, where ϵ_0 and ϵ_r are the vacuum and relative permittivities, respectively, allows us to estimate the lower limit of IX concentration $n_{IX} \geq 5 \times 10^{10} \text{ cm}^{-2}$ for $U_{pn} \leq -4.0$ V. The inset of Fig. 2 contains the integral PL intensity for $B_{||}=0$ and 20 T as a function of U_{pn} , normalized to $U_{pn}=0$. The integral intensity remains close to unity even for higher negative bias, when the radiative recombination lifetime of the IX is strongly enhanced. Hence, we can conclude that the nonradiative recombination rate is very small in comparison to the radiative one. The dominant radiative recombination and also the small full width at half maximum (FWHM) ~ 2 meV of the DX peak at 4.2 K (for IX FWHM=2.5–4 meV) are parameters that are characteristic for good quality samples, and thus the PL spectra can be compared to those published in Refs. 4 and 6.

Figure 3 summarizes the PL spectra measured in in-plane magnetic fields of up to $B_{||}=22$ T for $U_{pn}=-2.0$ and -4.0 V. The integral intensities of these spectra have been plotted in the inset of this figure. The magnetic field $B_{||}$ causes a blueshift of the IX peak, but no intensity degradation is present, contrary to previously published results.^{4–6} Moreover, the PL

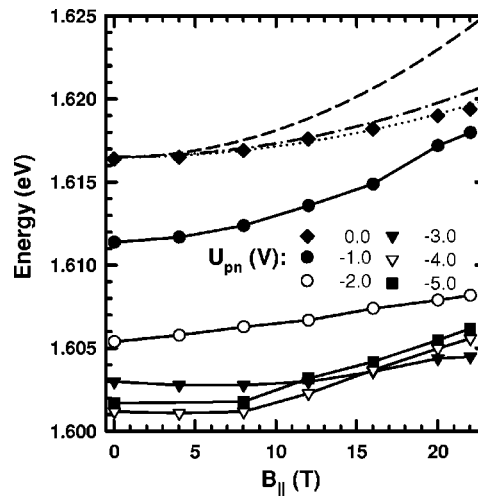


FIG. 4. The exciton peak energy for selected bias U_{pn} . The dotted line shows the parabolic DX shift $0.0065 \text{ meV/T}^2 \times B_{||}^2$. The dashed and dash-dotted lines represent the theoretical IX energy shift according to $e^2 d^2 B_{||}^2 / 2M$ for the exciton mass $0.21m_0$ and $0.42m_0$, respectively. Other lines serve as a guide for the eye only.

of direct excitons declines relatively to the IX peak. For comparison, we can estimate the Gaussian suppression of IX peak intensity according to the simple model⁴ sketched in the Introduction. However, we stress that its validity conditions are not fulfilled for our sample with a low nonradiative decay rate. The estimated intensity decrease at $B_{||}=20$ T then varies within an interval of 10^2-10^8 , due to the uncertainty in the exciton mass and the IX temperature. The values $M=0.42m_0$ and $0.21m_0$ (m_0 is the bare electron mass) were used for the exciton mass in Refs. 4 and 6, respectively, and in both cases in agreement with their experiments. The IX temperature is possibly higher than the lattice temperature $T_{latt}=4.2$ K, but we suppose that the temperature does not exceed 10 K, owing to high cooling rates of indirect excitons.²

We will now show that apart from the nonradiative and free IX recombination, another radiative recombination channel must be present to explain our measurements. As is shown in the insets of Figs. 2 and 3, the integral PL intensities are almost magnetic-field independent and are influenced only weakly by the applied electric field. Hence, the nonradiative recombination must be small. The probability of free IX radiative recombination with $K \approx 0$ is nearly magnetic-field independent⁴ and thus the intensity of the IX peak is governed predominantly by the number of IXs at the corresponding energy level. If no other radiative channel were present, an increase of the IX density n_{IX} by the factor $\exp(e^2 d^2 B_{||}^2 / 2Mk_B T)$ would be necessary to maintain the integral PL intensity constant. However, such a high IX density (more than 10^{12} cm^{-2} at $U_{pn} \leq -4.0$ V in higher magnetic fields) would cause a strong effective screening of the external electric field, resulting in a decrease of DQW tilting, and thus also in a strong blueshift of the IX peak. This is in contradiction with the experimentally determined IX maxima depicted in Fig. 4 for several values U_{pn} . Hence, the IX

luminescence observed in high in-plane magnetic fields cannot be related to the recombination of optically active free IXs (i.e., with the CM momentum $K \approx 0$) only. Therefore, another radiative recombination channel must be found. Although the repulsive interaction between IXs partially screens the potential fluctuations,² we suppose that the localization of the IXs plays a crucial role in the recombination process. In high magnetic fields, when the optical recombination of IX with a nonzero CM momentum is forbidden, the radiative recombination of localized IXs becomes dominant, whereas the nonradiative channel still seems to be negligible. The localized IX wave function is widely spread in the k space. Hence, the CM momentum conservation can be relaxed. The IX CM localization within the radius of 5 nm corresponds to the spread of wave function $\Delta K \approx 0.2 \text{ nm}^{-1}$ that is comparable with the shift $K_0 = edB_{\parallel}/\hbar$ of the IX dispersion parabola (1) induced by the in-plane magnetic field $B_{\parallel} \approx 20 \text{ T}$. So we assume that a certain number of IXs becomes localized and therefore optically active also in high magnetic fields. This localization seems to be present, although our sample shows properties characteristic for a high quality structure. We interpret this fact as a result of a very low nonradiative recombination rate that leads to an enhancement of IX lifetime and thus supports the IX localization. So, the very low nonradiative recombination rate in our structure seems to be responsible for results different from those published previously.⁴⁻⁶

A clearly noticeable feature of our luminescence spectra is the low-energy tail of the IX peak developing with increasing magnetic field. We suppose that it is related to lower-lying localized IX states. We think that this interpretation is also supported by the PL measurements in Ref. 6, where a strong damping of the (unbound) IX peak in higher magnetic fields was observed while the low-energy tail survived. However, this effect was not discussed in detail there.

Some attention should be paid to Fig. 4. The peak maximum shift for $U_{pn} = 0.0 \text{ V}$, i.e., for DX transition, is approximately quadratic in magnetic field, $\Delta E = 0.0065 \text{ meV/T}^2 \times B_{\parallel}^2$, and corresponds to the commonly observed diamagnetic shift^{4,5} of a DX. The shift for $U_{pn} = -1.0 \text{ V}$ is significantly higher, but this is caused by the mixing between the IX and DX states induced by B_{\parallel} . The PL maxima for $U_{pn} \leq -2.0 \text{ V}$ correspond to the pure IX transition. The measured IX peak shifts can be compared to theoretical curves for free IXs, simultaneously plotted in Fig. 4. These curves were obtained using the formula $e^2 d^2 B_{\parallel}^2 / 2M$ for the electron-hole distance $d = 22 \text{ ML}$ ($\approx 6.2 \text{ nm}$) and for two different values of the exciton mass^{4,6} $M = 0.42m_0$ and $0.21m_0$. For comparison, the DX transition was chosen as the reference energy. Evidently, the IX maxima do not follow this simple quadratic dependence. Instead, the observed IX shift at B_{\parallel} depends on the applied bias and is smaller for $U_{pn} = -2.0$ and -3.0 V than expected from theoretical curves. We relate this behavior to the IX localization and assume that the IX shift mainly represents the change in IX localization energy with the in-plane magnetic field. Also, slight but complex changes in the radiative recombination time of localized IX induced by the electric and magnetic fields can be expected. Because of the almost constant integrated PL intensity and the very

low nonradiative recombination, the lifetime change affects predominantly the IX density. This effect becomes important close to the saturation point $U_{pn} \approx -4.0 \text{ V}$, where the small changes in the IX density probably lead to different screenings of the external electric field and thus to different IX peak shifts. This can be clearly seen at $B_{\parallel} > 12 \text{ T}$, when the PL maxima for $U_{pn} = -4.0$ and -5.0 V appear at a higher energy than for $U_{pn} = -3.0 \text{ V}$. This blue shift of IX energy could be also supported by a possible charging of the DQW due to an exciton dissociation and electron tunneling out of the structure. Thus, although the shift for $U_{pn} = -4.0$ and -5.0 V is roughly comparable to the theoretical shift for the exciton with the mass $M = 0.42m_0$, we assume that it is of another origin than the plotted theoretical curve.

The shift of IX maxima with B_{\parallel} should be compared to the results published by Butov *et al.*⁹ They determined the IX mass as a function of the perpendicular magnetic field from the quadratic shift of the IX peak in the additionally applied magnetic field in the in-plane direction. They based the exciton mass evaluation on the simple relation $e^2 d^2 B_{\parallel}^2 / 2M$. In our case, owing to the localization of indirect excitons, the IX peak shift is influenced by the magnetic- and electric-field-induced changes of their localization energy and is smaller than the shift of free IX energy observed by Butov *et al.*⁹ Using of the simple formula would thus lead to an overestimation of the IX mass.

IV. CONCLUSION

We have shown that the IX peak can survive in PL spectra of good quality sample even in high in-plane magnetic fields. The low rate of nonradiative recombination supports the localization of long-living IXs that enables their radiative recombination also in high magnetic fields. On the contrary, the higher nonradiative recombination rate reduces the time available for the IX localization and thus effectively decreases the probability of radiative recombination in high in-plane magnetic fields.⁴

We conclude that the dominating radiative recombination of localized indirect excitons does not allow us to observe the quenching of IX luminescence and the quadratic shift of their energy in the in-plane magnetic field that were reported in Refs. 4-6 and 9. The possibility of an exciton dispersion engineering^{4,6,10} would then be limited in these kinds of samples.

ACKNOWLEDGMENTS

This work has been done within the research program, MSM113200002, financed by the Ministry of Education of the Czech Republic. M. O. acknowledges support from DAAD (German Academic Exchange Service, Bonn) and R. G., the support from the Alexander von Humboldt Foundation (AvH, Bonn, Germany). The high magnetic-field measurements were enabled by the program "Access to Research Infrastructure Action of the Improving Human Potential Programme" of EC.

*Electronic address: orlita@karlov.mff.cuni.cz

- ¹L. V. Butov, C. W. Lai, A. L. Ivanov, A. C. Gossard, and D. S. Chemla, *Nature (London)* **417**, 47 (2002).
- ²L. V. Butov, A. C. Gossard, and D. S. Chemla, *Nature (London)* **418**, 751 (2002).
- ³A. A. Gorbatsevich and I. V. Tokatly, *Semicond. Sci. Technol.* **13**, 288 (1998).
- ⁴A. Parlange, P. C. M. Christianen, J. C. Maan, I. V. Tokatly, C. B. Soerensen, and P. E. Lindelof, *Phys. Rev. B* **62**, 15 323 (2000).
- ⁵A. Parlange, P. C. M. Christianen, J. C. Maan, C. B. Soerensen, and P. E. Lindelof, *Phys. Status Solidi A* **178**, 46 (2000).
- ⁶L. V. Butov, A. V. Mintsev, Y. E. Lozovik, K. L. Campman, and A. C. Gossard, *Phys. Rev. B* **62**, 1548 (2000).
- ⁷J. Soubusta, R. Grill, P. Hlídek, M. Zvára, L. Smrčka, S. Malzer, W. Geißelbrecht, and G. H. Döhler, *Phys. Rev. B* **60**, 7740 (1999).
- ⁸M. Zvára, R. Grill, P. Hlídek, M. Orlita, and J. Soubusta, *Physica E (Amsterdam)* **12**, 335 (2002).
- ⁹L. V. Butov, C. W. Lai, D. S. Chemla, Y. E. Lozovik, K. L. Campman, and A. C. Gossard, *Phys. Rev. Lett.* **87**, 216804 (2001).
- ¹⁰K. Chang and F. M. Peeters, *Phys. Rev. B* **63**, 153307 (2001).